

# Computing dynamic responses of non-smooth dynamical systems

Marian Wiercigroch<sup>†</sup> & Ekaterina E. Pavlovskaja<sup>‡</sup>

*Centre for Applied Dynamics Research  
Department of Engineering, University of Aberdeen  
King's College, Aberdeen AB24 3UE, UK*

<sup>†</sup>M.Wiercigroch@eng.abdn.ac.uk

<sup>‡</sup>E.Pavlovskaja@eng.abdn.ac.uk

## 1. INTRODUCTION:

Non-smooth dynamical systems have numerous engineering applications. They are described by a set of piecewise smooth (linear or nonlinear) differential equations, and their direct numerical integration is usually very time consuming as points of discontinuities have to be determined with high precision. If a considered dynamical system is linear in all so-called subspaces, then an implicit global analytical solution can be given, providing the moments when non-smoothness occurs are determined. This leads to the necessity of solving nonlinear algebraic equations. To illustrate the non-smooth dynamical systems two engineering problems will be discussed in this paper.

First an impact oscillator with drift, which is used to model such processes as pipe driving, percussive drilling and ground moling, is considered [2]. This piecewise linear system can exhibit very complex behaviour including chaos, however it was obtained both theoretically and experimentally that the most interesting regimes from practical point of view (giving the best progression rates) are periodic. This has hinted a reduction of the original system to a low dimensional map. Initially an exact two-dimensional map has been formulated and analysed [3]. A further reduction to 1D approximate map is possible and will be discussed in the paper. Accuracy of the constructed maps was examined by comparing the dynamics responses with the exact solutions for a wide range of system parameters.

The second problem comes from rotordynamics, where nonlinear interactions between the rotor and the snubber ring will be studied. The results obtained from the developed mathematical model confronted with the experiment have shown a good degree of correlation.

## 2. VIBRO-IMPACT MOLING SYSTEM

As a first approximation, a vibro-impact moling system may be represented as an oscillating mass with a frictional visco-elastic slider [4]. This model defines the displacement of the mole (mass) and the soil (slider) which allows it to mimic the separation between the mole head and the front face of the hole. Dynamics of this model can be described as [2]

$$\begin{aligned}
 x' &= y, \\
 y' &= a \cos(s + \varphi) + b - P_1 P_2 (1 - P_3) (2\xi y + z - v) - P_1 P_3, \\
 z' &= P_1 y - (1 - P_1)(z - v)/2\xi, \\
 v' &= P_1 P_3 P_4 (y + (z - v - 1)/2\xi), \\
 s' &= \omega,
 \end{aligned} \tag{1}$$

where  $P_1 = H(x - z - e)$ ,  $P_2 = H(2\xi y + z)$ ,  $P_3 = H(2\xi + z - 1)$ ,  $P_4 = H(y)$ ,  $s = \omega\tau$ ,  $H(\cdot)$  is Heaviside step function,

and  $x$ ,  $z$  and  $v$  are displacements of the mass, the slider top and the slider bottom,  $y$  is the velocity of the mass,  $a$ ,  $\varphi$  and  $\omega$  are amplitude, phase shift and frequency of the external

excitation,  $b$  is external static force and  $e$  is a gap between the mass and the slider top in the initial moment of time,  $\tau = 0$ .

As it was reported in [5] by introducing a new system of co-ordinates  $(p, q, v)$  instead of  $(x, z, v)$ :  $p = x - v$ ,  $q = z - v$ , it is possible to decouple the oscillatory motion from the drift. In fact, in the new co-ordinates,  $p$  and  $q$  are displacements of the mass and the slider top relative to the current position of the slider bottom  $v$ . This decoupling procedure also allows to reduce the system dimension by one due to the fact that the bounded oscillations do not depend on the drift and it can be reconstructed afterwards.

The considered system can be at the time in one of the three following modes: *No contact* (the state space vector belongs to subspace  $\mathbf{X}_1$ , see Figure 1a), *Contact without progression* (the state space vector belongs to subspace  $\mathbf{X}_2$ ), and *Contact with progression* (the state space vector belongs to subspace  $\mathbf{X}_3$ ). The four dimensional flow of this system  $(\tau; p, y, q)$  can be locally three dimensional as during the contact modes relative displacements of the mass and slider top are not independent, i.e.  $p = q + e$ . This means that subspaces  $\mathbf{X}_2$  and  $\mathbf{X}_3$  are in fact planes, and consequently the borders  $\Pi\mathbf{X}_{1,2}$ ,  $\Pi\mathbf{X}_{2,3}$ ,  $\Pi\mathbf{X}_{3,2}$  and  $\Pi\mathbf{X}_{2,1}$  are lines. The cross-sections of the trajectories with these borders allow to define a two dimensional map, where the state of the system is fully described by value of  $\psi_n = \omega\tau_n + \varphi$  and velocity  $y_n$  at the moment of intersection  $\tau_n$ .

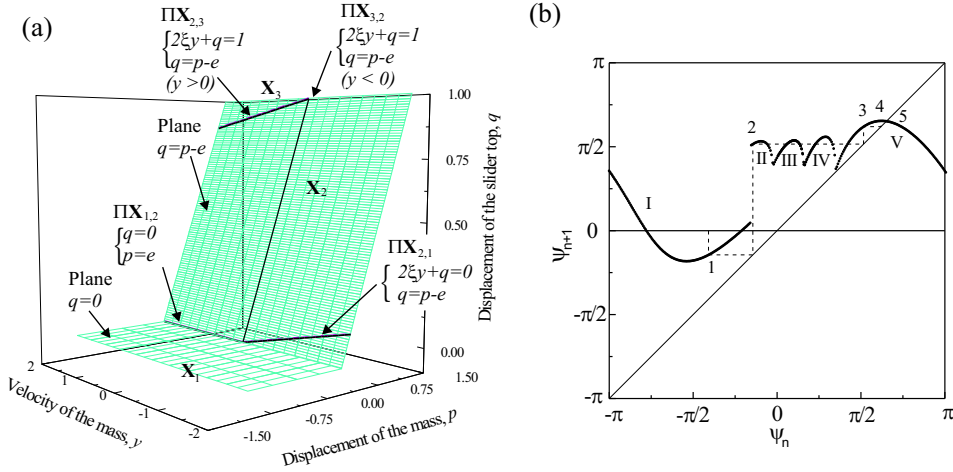


FIGURE 1. (a) The subspaces ( $\mathbf{X}_1$ – $\mathbf{X}_3$ ) and their borders ( $\Pi\mathbf{X}_{1,2}$ ,  $\Pi\mathbf{X}_{2,3}$ ,  $\Pi\mathbf{X}_{3,2}$  and  $\Pi\mathbf{X}_{2,1}$ ) for impact oscillator with drift; (b) Iteration of 1D approximate mapping converging to period one motion

Based on the four borders shown in Figure 1a, six local maps can be defined:

$$\begin{aligned} \mathbf{P}_1 : \Pi\mathbf{X}_{1,2} \rightarrow \Pi\mathbf{X}_{2,3}, \quad \mathbf{P}_2 : \Pi\mathbf{X}_{2,3} \rightarrow \Pi\mathbf{X}_{3,2}, \quad \mathbf{P}_3 : \Pi\mathbf{X}_{3,2} \rightarrow \Pi\mathbf{X}_{2,1}, \\ \mathbf{P}_4 : \Pi\mathbf{X}_{2,1} \rightarrow \Pi\mathbf{X}_{1,2}, \quad \mathbf{P}_5 : \Pi\mathbf{X}_{1,2} \rightarrow \Pi\mathbf{X}_{2,1}, \quad \mathbf{P}_6 : \Pi\mathbf{X}_{3,2} \rightarrow \Pi\mathbf{X}_{2,3}. \end{aligned} \quad (2)$$

At the beginning of the *Contact with progression* mode the four dimensional flow crosses the border  $\Pi\mathbf{X}_{2,3}$  and the system dynamics can be monitored using global two dimensional mapping

$$\mathbf{P} : \Sigma_2 \rightarrow \Sigma_2, \quad (3)$$

which maps  $y$  and  $\psi = \omega\tau + \varphi$  at the beginning of the *Contact with progression* mode to themselves,  $(y_{n+1}, \psi_{n+1}) = \mathbf{P}(y_n, \psi_n)$  [3]. The global map  $\mathbf{P}$  is an unknown combination of the local maps; and it can be equal to  $\mathbf{P} = \mathbf{P}_1 \circ \mathbf{P}_4 \circ \mathbf{P}_3 \circ \mathbf{P}_2$ ,  $\mathbf{P} = \mathbf{P}_6 \circ \mathbf{P}_2$  or  $\mathbf{P} = \mathbf{P}_1 \circ \mathbf{P}_4 \circ \mathbf{P}_5 \circ \mathbf{P}_4 \circ \mathbf{P}_3 \circ \mathbf{P}_2$  or another combination of local maps. For the harmonic external force the introduced two dimensional map is defined in the bounded region  $\psi_n \in (0, 2\pi)$ ,  $y_n \in (0, y^{max})$ , where  $y^{max}$  was estimated in [3].

The detailed analysis of the considered system reveals that a further reduction to 1D approximate map is possible. It has been found that the actual positions of the system at the end of

the *Contact with progression* mode (points belonging to the  $\Pi\tilde{\mathbf{X}}_{3,2}$ ) are very close to the point

$$\Pi\tilde{\mathbf{X}}_{3,2} = \{(\tau_i; p_i, y_i, q_i) \mid p_i = 1 + e, y_i = 0, q_i = 1\}, \quad (4)$$

and therefore approximate one dimensional map

$$\mathcal{P} : \Pi\tilde{\mathbf{X}}_{3,2} \rightarrow \Pi\tilde{\mathbf{X}}_{3,2} \quad (5)$$

can be introduced. The relation (5) maps the value of  $\psi$  at the end of the *Contact with progression* mode to itself,  $\psi_{n+1} = \mathcal{P}(\psi_n)$ .

The iterations of the proposed 1D approximate maps converging to period one regimes are shown in Figure 1b. In this figure each iterative step is marked by numbers 1,2,3, ... This map is presented in symmetrical region of  $\psi$ :  $\psi \in (-\pi, \pi)$  and as can be seen it has five distinctive smooth sub-regions marked by numbers from I to V. Each of these sub-regions corresponds to different types of system behaviour between two consecutive progression modes, i.e. for each of them the actual form of the map  $\mathcal{P}$  defined by a number of the *No contact* and *Contact without progression* modes is different. For the given set of parameters ( $a = 0.3$ ,  $b = 0.15$ ,  $\xi = 0.01$ ,  $\omega = 0.1$ ,  $\varphi = 0$ ,  $g = 0.02$ ), the system settles down on the period one orbit at  $\psi_n = 2.047$ . The transient motion before the settling down, however, may be very different depending on the chosen initial value of  $\psi_n$ .

### 3. ROTOR SYSTEM WITH A SNUBBER RING

Nonlinear interactions between the rotor and the snubber ring have been studied experimentally and theoretically. Figure 2a shows the experimental rig which comprises essentially two main parts, a rigid rotor (1), which is visco-elastically supported by four flexural rods (2), and excited by the out-of-balance mass (3), and a snubber ring (4), which is also elastically supporting using four compression springs. The rotor assembly consists of a mild steel rotor, running in two angular bearings. Holes (5) are drilled and tapped in both inner sleeves for the addition of imbalance weights. A pair of dampers (6) is attached to the rotor, one in each direction, to provide the system with heavier damping. The damping is assumed to be viscous type. Four flexural rods (2) are symmetrically clamped at one end to the outer bearing housing and at the other to a large support block. The support block (7) is in turn bolted to a large cast iron bed. The discontinuous stiffness is provided by a ring to which four compression springs (8), of much greater stiffness than that of the flexural rods, are symmetrically secured. The other ends of the springs are fixed to a large frame, clamped to the bed. The rotor runs inside the ring, with a radial clearance between the ring (4) and the outer bearing housing (1).

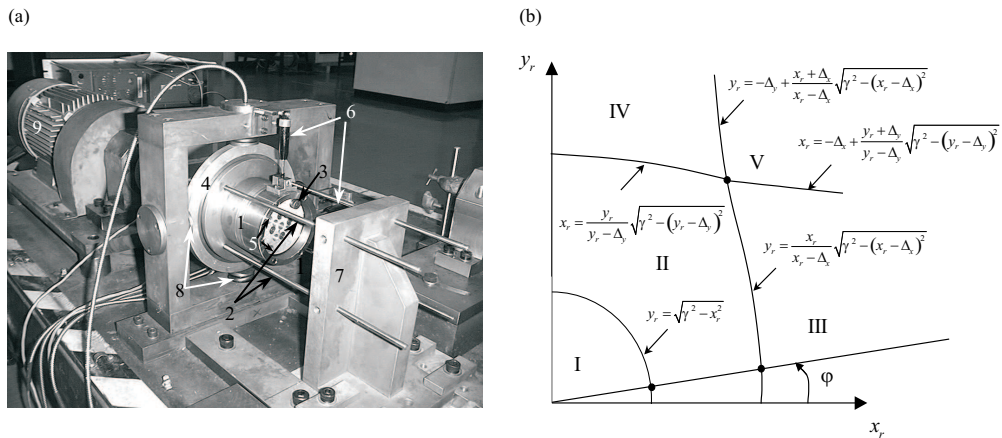


FIGURE 2. (a) Experimental rig of the investigated rotor system; (b) Regions of operation and their boundaries for the first quadrant of  $(x_r, y_r)$  plane

The rotor system with a preloaded snubber ring has been modelled as a two-degrees-of-freedom model [7]. The excitation is provided by an out-of-balance rotating mass. During operation

the rotor makes intermittent contact with the snubber ring. It is assumed that contact is non-impulsive, the snubber ring itself is massless and that the friction between the snubber ring and the rotor is neglected.  $x_r$  and  $y_r$ , and  $x_s$  and  $y_s$  represent horizontal and vertical displacements of the rotor and the snubber ring, respectively. The springs supporting the snubber ring are preloaded by  $\Delta_x$  in horizontal and  $\Delta_y$  in vertical directions respectively. There is a gap between the rotor and the snubber ring. Also in the initial position, the centre of the rotor is displaced from the centre of the snubber ring.

The system can operate in one of two following regimes: (a) no contact and (b) contact between the rotor and the snubber ring. In the latter case, existence of the preloading makes the dynamics of the system more complicated as the force acting from the snubber ring on the rotor depends on whether the displacement of the snubber ring exceeds the preloadings (in one or both directions) or not. Thus the following unique regimes of the system motion can be distinguished (see Figure 2b)

- I No contact between rotor and snubber ring.
- II Contact between the rotor and the snubber ring, where the both displacements of the snubber ring are smaller than the preloadings, i.e.  $|x_s| \leq \Delta_x$  and  $|y_s| \leq \Delta_y$ .
- III Contact between the rotor and the snubber ring, where the displacement of the snubber ring in the horizontal direction is larger than the preloading,  $|x_s| > \Delta_x$ , and in the vertical direction is smaller than preloading,  $|y_s| \leq \Delta_y$ .
- IV Contact between the rotor and the snubber ring, where the displacement of the snubber ring in the horizontal direction is smaller than the preloading,  $|x_s| \leq \Delta_x$ , and in the vertical direction is larger than preloading,  $|y_s| > \Delta_y$ .
- V Contact between the rotor and the snubber ring, where the displacements of the snubber ring are larger than the preloadings, i.e.  $|x_s| > \Delta_x$  and  $|y_s| > \Delta_y$ .

Equations of motion for this system were formulated and can be found in [7]. An extensive nonlinear dynamics analysis has been carried out by a combination of direct numerical integration and solving nonlinear algebraic equations defining the position of the snubber ring. Also a number of approximate methods based on linearization of the equation of motion at the moment of contact [6] were applied. To obtain approximate analytical solution, during contact regimes nonlinear functions were expanded in the Taylor series retaining only first order term, and for more complicated responses to increase level of accuracy the expansion procedure was repeated a few times during the contact.

A comparison between the theoretical and experimental results made by using bifurcation diagrams, phase portraits and Poincaré maps shows a good correlation between theory and experiments [8].

## REFERENCES

- [1] Wiercigroch, M. *Chaos, Solitons and Fractals* 11(15), **2000** 2429-2442.
- [2] Pavlovskaja, E.E., Wiercigroch, M. and Grebogi, C. *Physical Review E* 64, **2001** 056224.
- [3] Pavlovskaja, E.E., Wiercigroch, M. and Grebogi, C. *Physical Review E* 70, **2004** 036201.
- [4] Pavlovskaja, E.E., Wiercigroch, M., Woo, K.-C. and Rodger, A.A. *Meccanica* 38, **2003** 85-97.
- [5] Pavlovskaja, E. and Wiercigroch, M. *Chaos, Solitons and Fractals* 19 (1), **2004** 151-161.
- [6] Karpenko, E., Wiercigroch, M., Pavlovskaja, E.E and Cartmell, M.P. *International Journal of Mechanical Sciences* 44(3), **2002** 475-488.
- [7] Pavlovskaja, E.E., Karpenko, E.V. and Wiercigroch, M. *Journal of Sound and Vibration* 276(1-2), **2004** 361-379.
- [8] Karpenko, E.V., Wiercigroch, M., Pavlovskaja, E.E. and Neilson, R.D., Experimental verification of Jeffcott rotor model with preloaded snubber ring, submitted in October 2004.